Melanocortins and agouti-related protein modulate the excitability of two arcuate nucleus neuron populations by alteration of resting potassium conductances

Smith, Mark A.; Hisadome, Kazunari; Al-Qassab, Hind; Heffron, Helen; Withers, Dominic J.; Ashford, Michael L. J.

Published in:
Journal of Physiology

DOI:
10.1113/jphysiol.2006.119479

Publication date:
2007

Document Version
Publisher's PDF, also known as Version of record

Melanocortins and agouti-related protein modulate the excitability of two arcuate nucleus neuron populations by alteration of resting potassium conductances

Mark A. Smith[1], Kazunari Hisadome[1], Hind Al-Qassab[2], Helen Heffron[2], Dominic J. Withers[2] and Michael L. J. Ashford[1]

[1]*Neurosciences Institute, Division of Pathology and Neuroscience, Ninewells Hospital and Medical School, University of Dundee, Dundee, UK*
[2]*Centre for Diabetes and Endocrinology, Rayne Institute, University College London, London, UK*

The hypothalamic melanocortin system is crucial for the control of appetite and body weight. Two of the five melanocortin receptors, MC3R and MC4R are involved in hypothalamic control of energy homeostasis, with the MC4R having the major influence. It is generally thought that the main impact of the melanocortin system on hypothalamic circuits is external to the arcuate nucleus, and that any effect locally in the arcuate nucleus is inhibitory on proopiomelanocortin-expressing (POMC) neurons. In contrast, using current- and voltage-clamp recordings from identified neurons, we demonstrate that MC3R and MC4R agonists depolarize arcuate POMC neurons and a separate arcuate neuronal population identified by the rat insulin 2 promoter (RIPCre) transgene expression. Furthermore, the endogenous MC3R and MC4R antagonist, agouti-related protein (AgRP), hyperpolarizes POMC and RIPCre neurons in the absence of melanocortin agonist, consistent with inverse agonism at the MC4R. A decreased transient outward (I_A) potassium conductance, and to a lesser extent the inward rectifier (K_{IR}) conductance, underlies neuronal depolarization, whereas an increase in I_A mediates AgRP-induced hyperpolarization. Accordingly, POMC and RIPCre neurons may be targets for peptide transmitters that are possibly released locally from AgRP-expressing and POMC neurons in the arcuate nucleus, adding further previously unappreciated complexity to the arcuate system.

(Received 17 August 2006; accepted after revision 19 October 2006; first published online 26 October 2006)
Corresponding author M. Ashford: Division of Pathology and Neuroscience, Ninewells Hospital and Medical School, University of Dundee, Dundee DD1 9SY, UK. Email: m.l.j.ashford@dundee.ac.uk

Over a billion people worldwide are overweight with 300 million classified as obese (Bays, 2004). Recent research into the central regulation of energy homeostasis has focused on a prototypical hypothalamic arcuate nucleus (ARC) network (Cowley, 2003; Cone, 2005), containing two neuronal populations, those expressing neuropeptide Y (NPY), and proopiomelanocortin (POMC). NPY stimulates, and α-melanocyte-stimulating hormone (α-MSH – a *POMC* gene product) suppresses, food intake (Ramos *et al.* 2005). Agouti-related protein (AgRP) is predominantly localized to NPY neurons, is a natural antagonist of α-MSH on melanocortin 3 (MC3R) and melanocortin 4 (MC4R) receptors and stimulates a long-lasting increase in food intake (Hagan *et al.* 2000). The NPY/AgRP and POMC systems alter metabolic homeostasis by regulation of gene transcription, excitability and synaptic transmission (Cowley, 2003; Cone, 2005). They project to areas such as the paraventricular nucleus (PVN) and lateral hypothalamic area (LHA), where further integration occurs and outputs from these and the ARC extend to extra-hypothalamic centres. Hence, sites extrinsic to the ARC are thought to be where melanocortin receptors predominantly influence circuits responsible for energy homeostasis.

Alterations of the melanocortin pathway, predominantly via the MC4R, have a major influence on energy homeostasis. Global deletion of the *NPY* gene (Erickson *et al.* 1996) produces a weak phenotype in comparison to transgenes that target the melanocortin system. Notably the MC4R knockout mouse (Huszar *et al.* 1997) and mice overexpressing agouti (Fan *et al.* 1997)

 DOI: 10.1113/jphysiol.2006.119479

or AgRP (Graham *et al.* 1997) are obese. Furthermore, selective ablation of AgRP and POMC neurons induces anorexia and hyperphagia, respectively, (Gropp *et al.* 2005). The MC4R displays constitutive activity, which appears to be essential for body weight maintenance (Srinivasan *et al.* 2004). AgRP is an inverse agonist and suppresses the intrinsic activity of the MC4R (Haskell-Luevano & Monck, 2001), indicating that AgRP may increase food intake independently of melanocortin ligands. Moreover, approximately 5% of severe human obesity has been ascribed to MC4R deficiency (Farooqi *et al.* 2000), and the melanocortin system, including AgRP, is implicated in anorexia (Kas *et al.* 2003), cachexia (Lechan & Tatro, 2001) and type 2 diabetes (Bonilla *et al.* 2006).

Although melanocortin receptors are key elements in energy homeostasis control, relatively little is known about the electrophysiological properties of MC3R- and MC4R-expressing neurons in these hypothalamic circuits. Previous studies have shown that ARC NPY neurons are insensitive to the mixed MC3R and MC4R agonist, MTII (Roseberry *et al.* 2004) and POMC neurons are inhibited by an MC3R agonist (Cowley *et al.* 2001). In addition to these neurons, an independent ARC neuronal population, identified by the rat insulin 2 promoter (RIPCre) transgene expression was demonstrated to differ from POMC neurons in its response to insulin and leptin. POMC neurons are hyperpolarized by insulin and depolarized by leptin, whereas RIPCre neurons are depolarized by insulin but are insensitive to leptin (Choudhury *et al.* 2005). Additionally, the mixed MC3R/MC4R agonist MTII depolarized RIPCre neurons. Consequently, we have investigated the mechanisms by which melanocortin agonists and AgRP alter the excitability of POMC and RIPCre neurons. We show here that melanocortin agonists depolarize and induce excitation of both POMC and RIPCRe neurons and that AgRP inhibits both neuron populations by membrane hyperpolarization.

Methods

Hypothalamic slice preparation

As previously described (Choudhury *et al.* 2005), we have used two Cre recombinase transgenic lines, RIPCre and POMCCre and intercrossed these with the ZEG indicator mouse to generate mice expressing green fluorescent protein (GFP) in selective hypothalamic neuronal populations. All procedures conformed to the UK Animals (Scientific Procedures) Act 1986, and were approved by our institutional ethical review committee. RIPCreZEG and POMCCreZEG mice (8-16 weeks old) were killed by cervical dislocation, the brain rapidly removed and submerged in an ice-cold slicing solution containing (mM): KCl 2.5, NaH_2PO_4 1.25, $NaHCO_3$ 28, $CaCl_2$ 0.5, $MgCl_2$ 7, D-glucose 7, ascorbate 1, pyruvate 3 and sucrose 235, equilibrated with 95% O_2–5% CO_2 to give a pH of 7.4. Hypothalamic coronal slices (350 μm), containing the ARC, were cut using a Vibratome, transferred and kept at room temperature (22–25°C) in an external solution containing (mM): NaCl 125, KCl 2.5, NaH_2PO_4 1.25, $NaHCO_3$ 25, $CaCl_2$ 2, $MgCl_2$ 1, D-glucose 10, D-mannitol 15, ascorbate 1 and pyruvate 3, equilibrated with 95% O_2–5% CO_2; pH 7.4, ~320 mosmol l^{-1}.

Electrophysiology

Individual arcuate neurons were identified by epifluorescence and differential interference contrast optics using an upright Zeiss Axioskop-2 FS plus microscope. Slices were continually perfused with a modified external solution (0.5 mM $CaCl_2$ and 2.5 mM $MgCl_2$, no ascorbate and pyruvate) at a flow rate of 5–10 ml min^{-1} and a bath temperature of 33°C. For experiments in high-potassium solution, the normal external solution was replaced by a solution containing (mM): NaCl 130, KCl 20, $CaCl_2$ 0.5, $MgCl_2$ 2.5, D-glucose 10, D-mannitol 15 and Hepes 10; pH 7.4, ~320 mosmol l^{-1}. Patch-clamp recordings were performed using borosilicate patch pipettes (4–8 MΩ) filled with an internal solution containing (mM): potassium gluconate 130, KCl 10, EGTA 0.5, Hepes 10, NaCl 1, $CaCl_2$ 0.28, $MgCl_2$ 3, Na_2ATP 3, Tris-GTP 0.3 and phosphocreatine 14; pH 7.2, ~310 mosmol l^{-1}. Whole-cell series resistance (R_s) was compensated using an Axopatch 200B amplifier in current- (I_{fast}) and voltage-clamp modes (R_s, 30–60 and 10–30 MΩ, respectively). Note that any remaining uncompensated capacitance, produced by the voltage steps, was digitally subtracted in Igor Pro using a −90 mV voltage step as a template. Voltage and current commands were manually or externally driven using pCLAMP 9.2 software and injected into neurons via the patch-clamp amplifier. Under current clamp, hyperpolarizing current pulses (5–20 pA, 200 ms, at a frequency of 0.05 Hz) were used to monitor input and series resistance. Whole-cell currents and voltages were filtered at 5 and 2 kHz, respectively, and digitized at 50 kHz using pCLAMP 9.2 software. Miniature excitatory postsynaptic currents (mEPSCs) were recorded in a standard external solution (2 mM $CaCl_2$ and 1 mM $MgCl_2$) and in the presence of (+)bicuculline (20 μM), whereas miniature inhibitory postsynaptic currents (mIPSCs) were recorded in the presence of 2 mM kynurenic acid. Neurons were voltage clamped at −70 mV using a CsCl-based (130 mM) internal solution containing 5 mM QX314 to block regenerative sodium spikes. Unitary events of uniform rise and decay kinetics were identified by the template detection function in Clampex 9.2 and were analysed for peak amplitude and frequency. All data were stored unsampled on digital audio tape for off-line analysis

using Clampex 9.2 or Igor Pro. Membrane potentials were either replayed unsampled on an EasyGraph TA240 chart recorder (Gould), or digitized and imported into Adobe illustrator for illustration purposes.

Unless stated otherwise, drugs were added to the external solution and applied to the slice via the perfusion system. Occasionally, drugs were locally applied using a broken-tipped pipette (~4 μm diameter) positioned above the recording neurons, as previously described (Choudhury *et al.* 2005). At least 10 min of stable control data were recorded before the application of any drug, and, wherever possible, complete reversibility upon washout was sought. However, some responses appeared not to reverse completely as commonly found with peptides, even following extensive washout ($\geq$1 h). Note that neuronal integrity was assessed by all of the following: small holding current ($\leq$20 pA at $-$70 mV) when voltage clamped, high input resistance ($\geq$1 GΩ), large amplitude rebound spikes, the ability to fire and lack of obvious morphological deterioration (i.e. lack of blebbing and nucleus not visually present).

Chemicals

Kynurenic acid, (+)bicuculline, tetraethylammonium chloride (TEA), tolbutamide, 4-aminopyridine (4-AP), nimodipine, QX314 and mibefradil dihydrochloride were purchased from Sigma (Dorset, UK). Neuropeptide Y (NPY), JKC363, SHU9119, AgRP (82–131)-amide, MC4R agonist (cyclo(β-Ala-His-D-Phe-Arg-Trp-Glu)-NH_2) and melanotan II (MTII) were obtained from Phoenix Pharmaceuticals Inc. (Belmont, CA, USA). Tetrodotoxin (TTX), r-tertiapin-Q, r-heteropodatoxin-2 (HpTX) and ω-conotoxin GVIA were purchased from Alomone Laboratories Ltd (Jerusalem, Israel). D-Trp^8-γ-MSH was a gift from Dr V. J. Hruby (University of Arizona).

Statistics

Statistical significance was determined on all neurons examined within a data set, using Student's two-tailed paired *t* test. However, as described by Cowley *et al.* (2001), we found that POMC neuronal responsiveness was not homogeneous. Therefore, as described by Dhillon *et al.* (2006), we divided responding neurons from non-responding neurons based on the criterion that the change (in membrane potential or current amplitude) induced by the drug challenge was $\pm$ three times the standard deviation prior to drug addition. The mean $\pm$ standard error of these responses is presented, with the number of cells studied.

Results

Whole-cell current-clamp recordings were made from GFP-positive hypothalamic arcuate neurons from RIPCreZEG and POMCCreZEG mice. Consistent with previous reports (Cowley *et al.* 2001; Acuna-Goycolea & van den Pol, 2005; Choudhury *et al.* 2005; Plum *et al.* 2006), under control conditions, arcuate neurons were characterized by high mean input resistances (RIPCre, 1.9 ± 0.2 GΩ, $n = 62$; POMC, 1.5 ± 0.05 GΩ, $n = 50$) and spontaneously fired sodium-mediated action potentials from a mean resting membrane potential (V_m, range -40 to -60 mV) of -50 ± 1 mV (RIPCre; $n = 62$) and -50 ± 1 mV (POMC; $n = 50$).

Selective MC3R and MC4R agonists depolarize POMC and RIPCre neurons

In contrast to a previous report (Cowley *et al.* 2001), the selective MC3 receptor agonist (D-Trp^8-γ-MSH, 10–50 nM) depolarized ($P < 0.05$, $n = 11$) POMC neurons (Fig. 1*A*) by $+5.9 \pm 1.2$ mV ($n = 7$ out of 11), although a lower concentration (5 nM) had no effect on POMC neuronal excitability ($n = 5$, data not shown). D-Trp^8-γ-MSH (10–20 nM) also depolarized RIPCre neurons (Fig. 1*B*) by $+9.6 \pm 3.2$ mV ($P < 0.05$, $n = 5$ out of 5). Moreover, the selective MC4 receptor agonist cyclo(β-Ala-His-D-Phe-Arg-Trp-Glu)-NH_2 (10–20 nM; Bednarek *et al.* 2001) depolarized a majority of POMC neurons (Fig. 1*C*, $P < 0.05$, $n = 6$) by $+2.0 \pm 0.4$ mV ($n = 4$ out of 6) and RIPCre neurons (Fig. 1*D*, $P < 0.05$, $n = 17$) by $+5.4 \pm 1.2$ mV ($n = 7$ out of 17).

AgRP and SHU9119 oppose the actions of melanocortin agonists

As the response to the MC4R agonist was unexpected, we examined whether AgRP could oppose the constitutive receptor activity associated with this receptor type (Haskell-Luevano & Monck, 2001). In the absence of bath-applied melanocortin agonist and consistent with its inverse agonist properties, AgRP (10–20 nM) hyperpolarized RIPCre (change in V_m (ΔV_m), -18.3 ± 4.8 mV, $P < 0.05$, $n = 4$ out of 4) and POMC (ΔV_m, -2.4 ± 0.7 mV, $n = 5$ out of 10; $P < 0.05$, $n = 10$) neurons (Fig. 2*A* and *B*). However, AgRP did not significantly affect input resistance (% of control: RIPCre, 78 ± 15%; POMC, 93 ± 7%; $P > 0.1$). Furthermore, AgRP did not exert its neuromodulatory effects on these ARC neurons indirectly by alteration of synaptic activity as RIPCre neuron membrane potential was hyperpolarized by AgRP (Fig. 2*C*; $n = 3$ out 3) in the presence of TTX (0.5 μM).

We have previously shown that the mixed MC3R and MC4R agonist, melanotan II (MTII) depolarizes RIPCre neurons (Choudhury *et al.* 2005; Fig. 2*D*, $n = 7$ out of 13). To confirm that MTII-induced depolarization was due to the activation of MC3R and MC4R, we attempted to block the MTII response by prior application of the neutral MC3R and MC4R antagonist

SHU9119. Accordingly, SHU9119 (10–25 nM) prevented MTII-induced depolarization of RIPCre neurons (SHU9119, -45 ± 4 mV; SHU9119 + MTII, -46 ± 3 mV; $n = 3$ Fig. 2*E*) although, overall SHU9119 alone ($P < 0.05$, $n = 8$) hyperpolarized (Fig. 2*F*) RIPCre neurons (ΔV_m, -8.0 ± 2.8 mV, $n = 5$). MTII also depolarized POMC neurons ($P < 0.05$, $n = 11$) by a similar magnitude to RIPCre neurons (ΔV_m, $+5.2 \pm 1.1$ mV, $n = 5$ out 11) and this effect was prevented by SHU9119 (SHU9119, -55 ± 3 mV; SHU9119 + MTII, -55 ± 3 mV; $n = 5$, Fig. 2*G*). In contrast to SHU9119, application of the selective MC4R antagonist JKC363 (10–20 nM) had no effect on the membrane potential of RIPCre neurons, but did reverse the depolarization ($P < 0.05$, $n = 10$) induced by the selective MC4R agonist (Fig. 2*H*). The MC4 receptor agonist depolarized RIPCre neurons by $+4.4 \pm 1.6$ mV ($P < 0.05$, $n = 10$) and the subsequent application of JKC363, in the continuous presence of MC4R agonist, repolarized these neurons by -4.4 ± 1.6 mV ($P < 0.05$), although again a significant delay in reversibility was observed (20–80 min). These data suggest that SHU9119 may possess some intrinsic inverse agonist activity independent of MC4R.

MTII and AgRP directly modulate POMC and RIPCre neuronal activity

While the effects of MTII (Choudhury *et al.* 2005) and AgRP were reproducible in the presence of TTX, it is possible that spontaneous miniature synaptic events (that are insensitive to TTX; Roseberry *et al.* 2004) are modulated by these peptides and contribute to the responses. Thus, the frequency and amplitude of spontaneous mIPSCs and mEPSCs were recorded in the absence and presence of bath and/or locally applied MTII. The frequencies of these spontaneous events were not affected by 100 nM MTII in RIPCre (mIPSC: control, 0.6 ± 0.2 Hz; MTII, 0.4 ± 0.1 Hz; $n = 4$, Fig. 3*A*; mEPSC: control, 4.1 ± 1.3 Hz; MTII, 4.1 ± 1.2 Hz; $n = 5$, Fig. 3*B*) and POMC (mIPSC: control, 0.5 ± 0.1 Hz; MTII, 0.7 ± 0.1 Hz; $n = 5$, Fig. 3*E*; mEPSC: control, 0.9 ± 0.2 Hz; MTII, 0.4 ± 0.1 Hz; $n = 5$, Fig. 3*F*) neurons. Moreover, the cumulative frequency–amplitude distributions did not differ between control events and those recorded in the presence of MTII for mEPSCs or mIPSCs in RIPCre neurons (Fig. 3*C* and *D*) or for mEPSCs in POMC neurons (Fig. 3*G*). However, in POMC neurons, mIPSC amplitude was reversibly increased by MTII (change in amplitude, $+6.1 \pm 0.9$ pA, $n = 5$, $P < 0.05$) and the cumulative frequency distribution shifted in the presence of MTII (Fig. 3*H*). These data indicate that MTII increases $GABA_A$ receptor tone on POMC neurons, as previously reported (Cowley *et al.* 2001). In contrast, the mechanism of action appears to differ, such that D-Trp^8-γ-MSH was reported to increase mIPSC frequency (Cowley *et al.* 2001), whereas in this study MTII increased synaptic amplitude.

To provide additional evidence for a direct (i.e. non-synaptic) effect of MTII and AgRP, the signalling pathway between receptor and ion channel was blocked in the postsynaptic neuron. Melanocortin receptors are members of the G-protein-coupled receptor family and have been reported to couple in a stimulatory manner to cAMP (Wikberg, 1999). Thus, we examined the effect of an inhibitor of cAMP-mediated outputs (Rp-cAMP) on electrical actions of both MTII and AgRP on RIPCre and POMC neurons. Neither the membrane potential

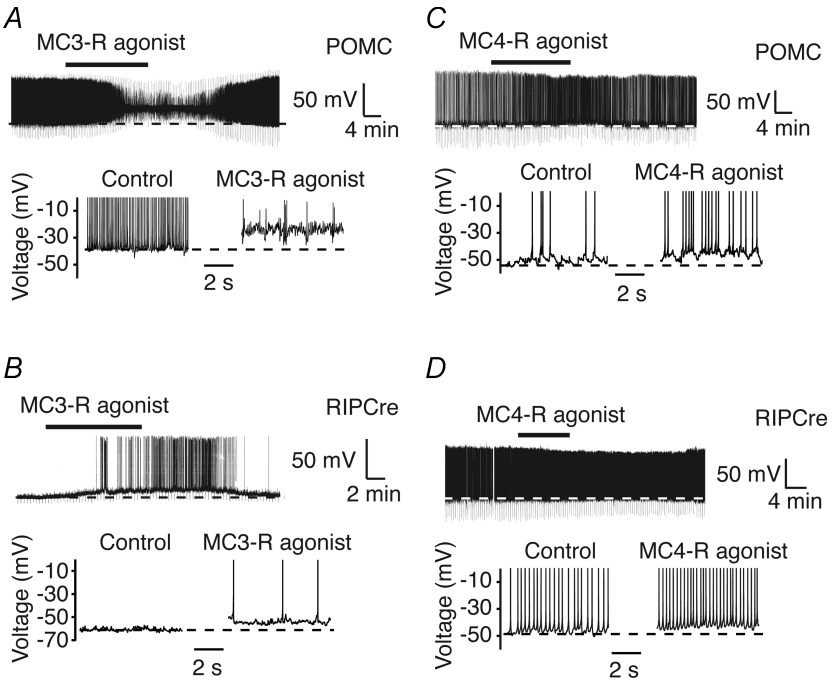

Figure 1. Selective MC3R and MC4R agonists depolarize POMC and RIPCre neurons
Current-clamp recordings were made from POMC (*A* and *C*) and RIPCre (*B* and *D*) neurons in the absence and presence of a selective MC3R (10 nM D-Trp^8-γ-MSH; *A* and *B*) or MC4R (10 nM cyclo(β-Ala-His-D-Phe-Arg-Trp-Glu)-NH_2; *C* and *D*) agonist. MC3R or MC4R activation results in POMC and RIPCre neuron depolarization, as demonstrated by the expanded sections shown underneath this and subsequent figures. Note that the large reversible depolarization induced by the MC3R agonist (*A*) produces significant spike amplitude attenuation.

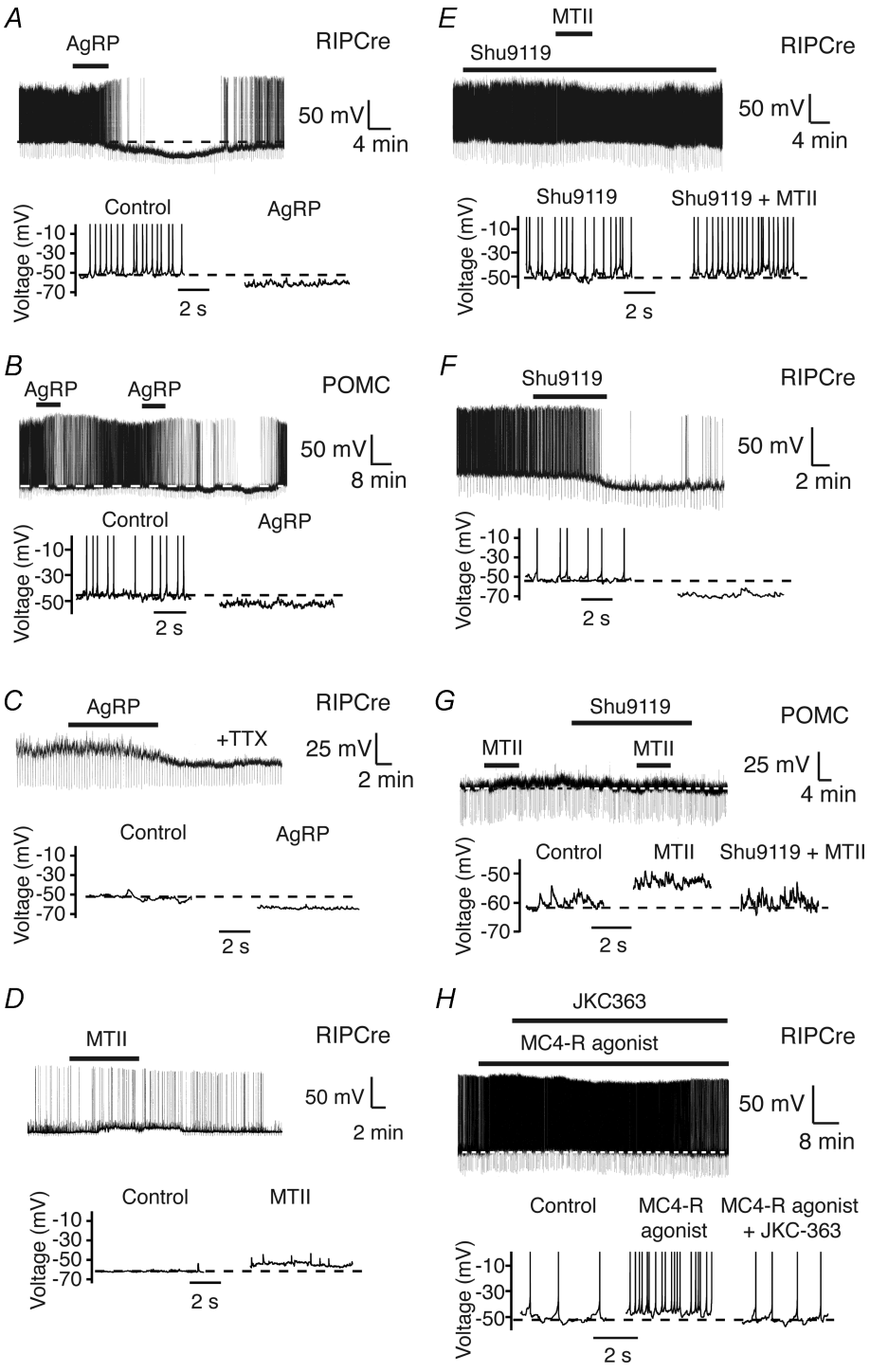

Figure 2. AgRP and melanocortin (MC) receptor antagonists oppose or block the actions of MC receptor agonists

RIPCre (*A*) and POMC (*B*) neurons are hyperpolarized by 10 nM AgRP, applied as denoted above the traces. *C*, AgRP hyperpolarizes RIPCre neurons in the presence of 0.5 μM TTX. RIPCre and POMC neurons are depolarized by the mixed MC3R/MC4R agonist MTII (100 nM; *D* and *G*) and this action is prevented by prior application of SHU9119 (20 nM; *E* and *G*). *F*, the majority of RIPCre neurons respond to SHU9119 alone by hyperpolarization. *H*, a selective MC4R agonist (20 nM) depolarizes RIPCre neurons, an action that is reversed by the presence of a selective MC4R receptor antagonist (20 nM, JKC363).

nor the spike frequency was altered by application of 100 nM MTII (control, -46 ± 2 mV; MTII, -45 ± 2 mV; control, 4.3 ± 1.5 Hz; MTII, 4.5 ± 1.0 Hz, $n = 6$ out of 6) or 10 nM AgRP (control, -47 ± 2 mV; AgRP, -46 ± 3 mV; control, 2.9 ± 0.8 Hz; AgRP, 3.0 ± 0.4 Hz, $n = 6$ out of 6) when 100 μM Rp-cAMP was present in the recording pipette solution (data not shown), suggesting that MTII has a direct effect on these neurons via MC3 and MC4 receptors coupling to adenylate cyclase.

Block of K^+ channels prevents MTII depolarization

As both POMC and RIPCre neurons displayed responses to melanocortin-selective ligands, which were indistinguishable from one another qualitatively, we did not discriminate between these populations when examining the mechanisms underlying these electrical changes, and consequently utilized MTII as agonist. Initially, we attempted to block the depolarizing response of MTII by the presence, in the bath solution, of various heavy metal cations (0.1–1 mM Gd^{3+}, La^{3+}, Cs^+, Cd^{2+} or Ni^{2+}), which block various non-selective cation and calcium channels (Hille, 2001). However, these and indeed more selective calcium channel blockers such as ω-conotoxin GVIA (100 nM), nimodipine (10 μM) and mibefradil (10 μM) did not alter the membrane potential or prevent MTII-induced depolarization of RIPCre neurons (data not shown). These data, while not conclusive, indicate that calcium and non-selective cation conductances are unlikely to be responsible for the MTII-induced depolarization. Thus, we assessed whether blocking potassium conductance could mimic or prevent the depolarization elicited by MTII on ARC neurons.

The presence of the ATP-sensitive potassium (K_{ATP}) channel inhibitor tolbutamide (200 μM) did not significantly affect membrane potential and failed to prevent depolarization of RIPCre neurons by 100 nM MTII ($n = 3$ out of 3; data not shown). Ba^{2+} (100 μM), a non-selective inward rectifier potassium (K_{IR}) channel blocker (Takano & Ashcroft, 1996; Liu *et al.* 2001), induced a small depolarization of RIPCre and POMC neurons (Fig. 4*A*) by $+2.5 \pm 0.5$ mV ($n = 4$ out of 4, $P < 0.05$). The voltage-dependent transient outward potassium ('I_A-type' currents) channel blocker (Wang *et al.* 1996),

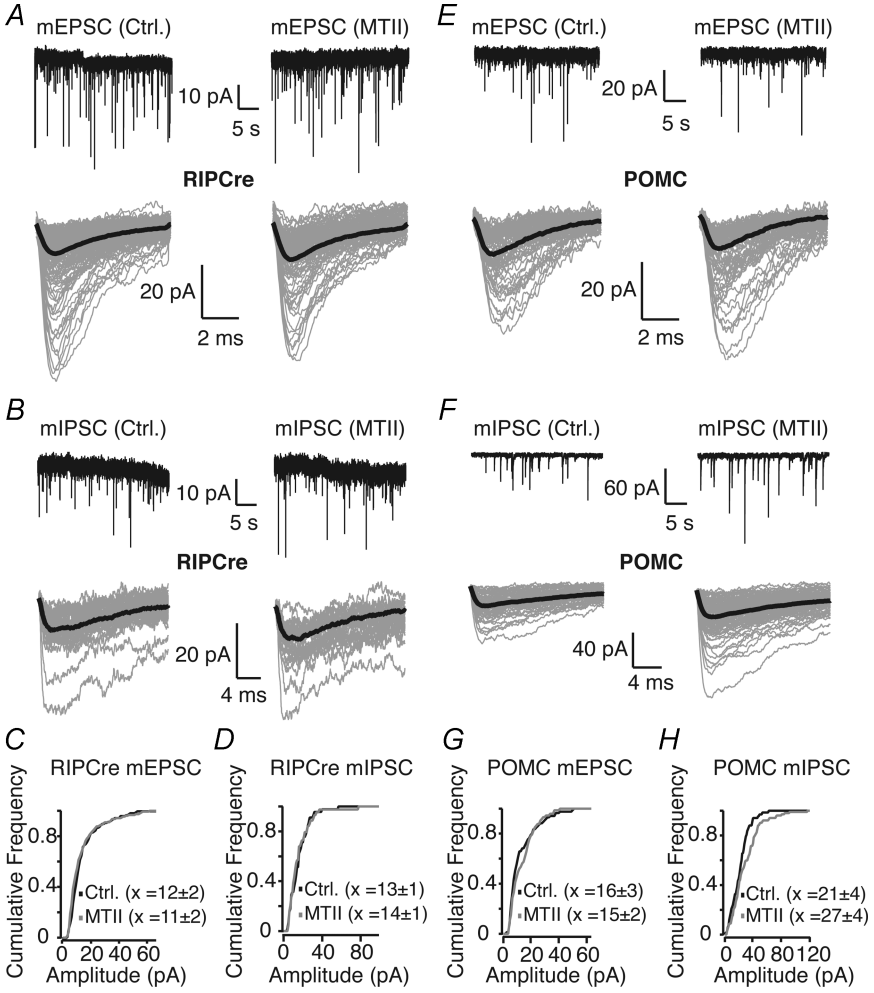

Figure 3. Effects of MTII on spontaneous synaptic events
RIPCre (*A–D*) and POMC (*E–H*) neurons were voltage clamped at −70 mV using a CsCl-based internal solution. Miniature excitatory (*A* and *E*) postsynaptic currents (mEPSC) were recorded in the presence of 20 μM (+)bicuculline, whereas miniature inhibitory postsynaptic currents (mIPSC; *B* and *F*) were recorded in the presence of 2 mM kynurenic acid. Under these recording conditions, both inhibitory and excitatory currents are shown as downward deflections, as demonstrated by the representative traces shown in *A*, *B*, *E* and *F*. Note that co-application of (+)bicuculline and kynurenic acid blocked all synaptic events (data not shown). Synaptic currents were recorded in the absence (left) and presence (right) of 100 nM MTII, as indicated. Superimposed synaptic events are shown underneath in grey and composite traces from between 50 and 150 events are shown in black. Representative amplitude–cumulative frequency histograms from recordings shown above are shown for mEPSC and mIPSC in RIPCre (*C* and *D*, respectively) and POMC (*G* and *H*, respectively) neurons.

4-AP (4 mM) depolarized RIPCre and POMC neurons by $+5.6 \pm 0.5$ mV ($P < 0.05$, $n = 5$ out of 5; Fig. 4*B*). These actions of Ba^{2+} and 4-AP were reproducible in the presence of inhibitors of glutamatergic (kynurenic acid) and GABAergic ((+)bicuculline) fast neurotransmission (data not shown). Consequently, hyperpolarizing current was injected into neurons in the presence of either Ba^{2+} or 4-AP to reset the membrane potential to the preblocker value prior to challenge with MTII (see Fig. 4*B* and *C*). Subsequent application of 100 nM MTII, in the presence of either Ba^{2+} (control, -52 ± 2 mV; Ba^{2+}, -52 ± 2 mV; $n = 4$ out of 4) or 4-AP (control, -57 ± 4 mV; 4-AP, -58 ± 6 mV; $n = 4$ out of 4) alone did not affect the resting membrane potential (Fig. 4*A* and *B*). Although Ba^{2+} was difficult to wash out from the slice, on the occasions where clear reversibility was obtained, re-application of 100 nM MTII induced a depolarizing response (e.g. Fig. 4*A*). Thus, the presence of either Ba^{2+} or 4-AP alone is capable of preventing neuron depolarization by 100 nM MTII, although MTII increased spike frequency from control by $69 \pm 20\%$ ($n = 4$, $P < 0.05$) and $36 \pm 5\%$ ($n = 4$, $P < 0.05$) in the presence of 4-AP and Ba^{2+}, respectively (Fig. 4*A* and *B*). However, in the combined presence of Ba^{2+} and 4-AP, 100 nM MTII was unable to alter the membrane potential (control, -55 ± 2 mV; MTII, -55 ± 4 mV, $n = 5$ out of 5) or firing frequency (control, 3.4 ± 0.5 Hz; MTII, 3.6 ± 0.7 Hz, $n = 5$) of POMC neurons (Fig. 4*C*), suggesting that both conductances (the transient outward current (henceforth termed I_A for convenience) and K_{IR}) contribute to the MTII response.

MTII and AgRP have opposing actions on K^+ conductances

In order to identify the potassium conductance modulated by MTII and AgRP, RIPCre neurons were voltage clamped in an external solution containing 10 μM bicuculline, 2 mM kynurenic acid and 1 μM TTX to block synaptic transmission and regenerative Na^+ spikes. Neurons were held at -70 mV and voltage pulses (500 ms duration) were stepped from -90 to -10 mV in 5 mV increments, with a 5 ms prepulse stepped to -170 mV (5 ms duration) to deactivate voltage-dependent potassium conductances (Fig. 5*A*). Initial studies with an external calcium concentration of 0.5 mM, 40 mM external tetraethylammonium (TEA) and internal K^+ replaced by Cs^+ (in order to inhibit potassium conductance), demonstrated that no significant calcium current could be observed (data not shown). In contrast, with normal external saline and potassium gluconate in the electrode solution, depolarizing command potentials (above -45 mV) elicited outward current, characterized by an initial rapid transient component that inactivated to reveal an underlying steady-state current (Fig. 5*B*).

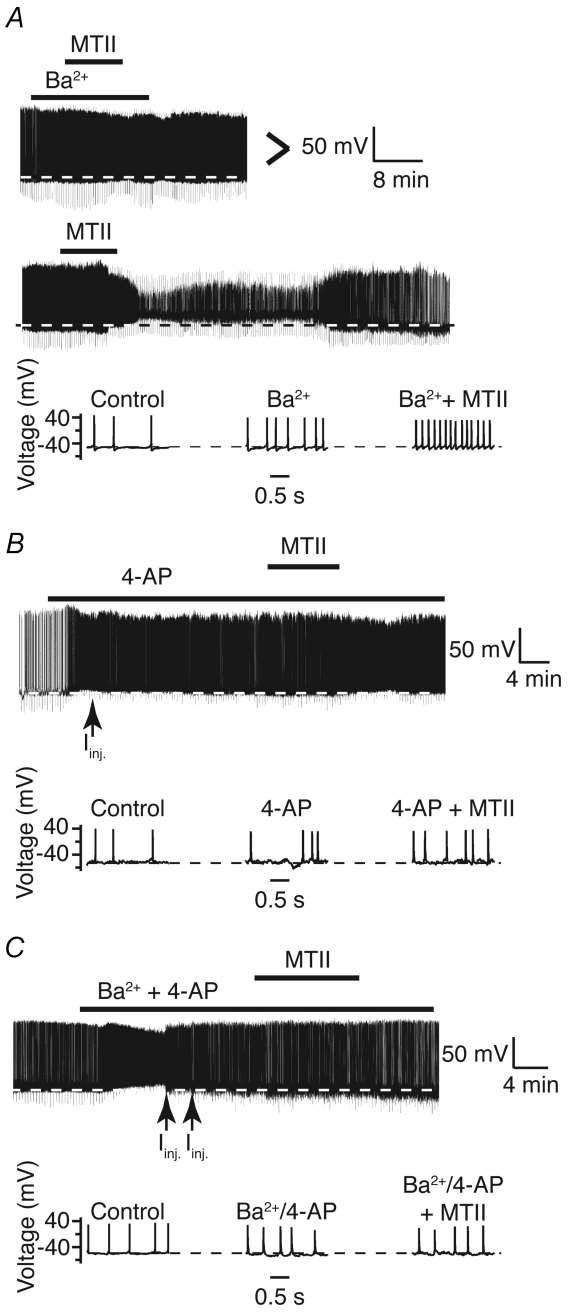

Figure 4. Ba^{2+} and 4-AP occlude MTII depolarization of RIPCre and POMC neurons
A, representative current-clamp recording from an RIPCre neuron showing that application of 100 μM Ba^{2+} prevents 100 nM MTII-induced depolarization, although there was an increase in firing frequency (as shown in the expanded sections underneath). Washout of the Ba^{2+} allowed recovery of the MTII-induced depolarizing response, with significant spike amplitude attenuation. > represents continuity of the voltage trace. *B*, 4 mM 4-AP caused depolarization of RIPCre neurons. Following injection of current ($I_{inj.}$) to restore the membrane potential, MTII was unable to induce significant depolarization, though firing frequency was increased. *C*, combined application of Ba^{2+} (100 μM) and 4-AP (4 mM) resulted in neuron (POMC) depolarization and on subsequent restoration of the membrane potential by current injection; application of MTII had no effect on membrane potential or firing frequency.

Such current kinetics are indicative of the I_A and delayed rectifier (I_K) potassium conductances, respectively. To confirm this interpretation we examined the effect of the I_A channel blocker 4-AP (4 mM). Accordingly, at −10 mV, 4-AP blocked the peak current by 56 ± 6% ($P < 0.05$, $n = 4$ out of 4) but also partially blocked the steady-state (measured at the end of the pulse) current (Fig. 5*B*) by 28 ± 6% ($P < 0.05$, $n = 4$ out of 4). Application of 40 mM TEA resulted in a 68 ± 4% ($n = 4$ out of 4, $P < 0.05$) depression in the amplitude of the delayed rectifier current (data not shown).

Local application of MTII above the recorded neuron depressed I_A peak amplitude at all voltages where a significant outward current could be observed (Fig. 5*C*). This is more clearly shown for single currents elicited by depolarization to −20 mV, where 100 nM MTII reduces

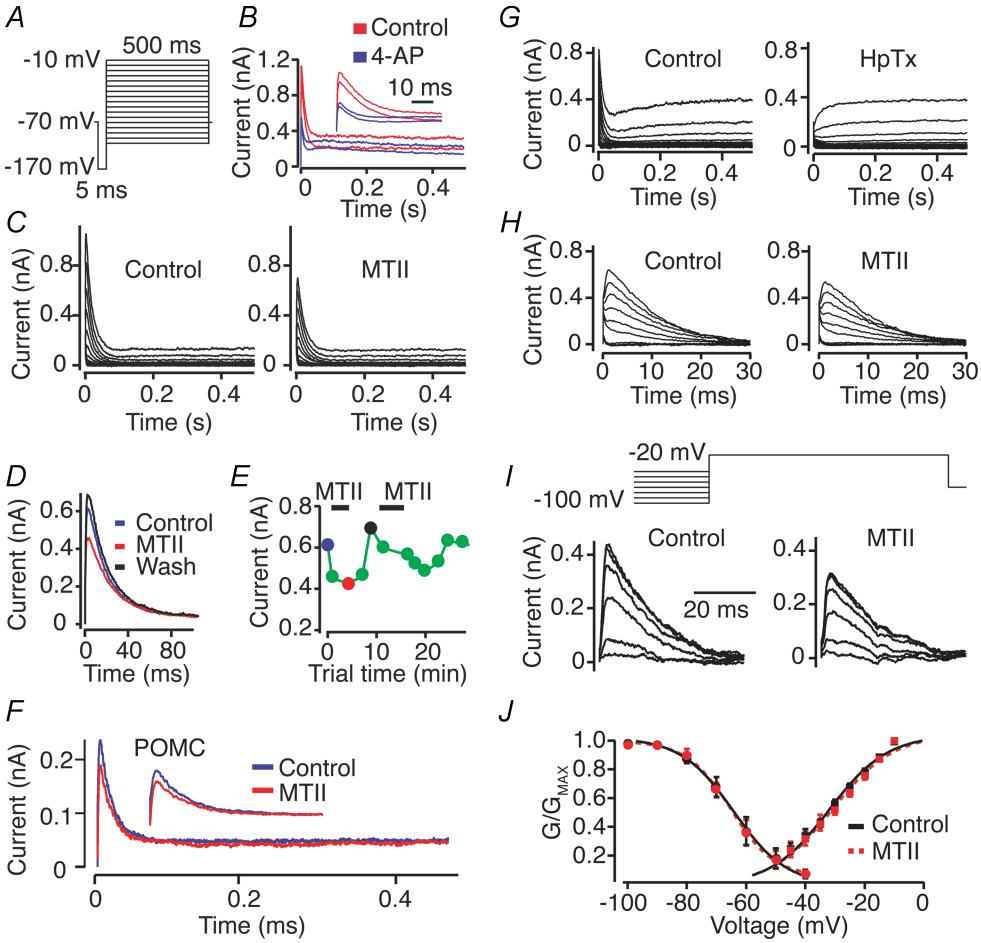

Figure 5. The transient voltage-gated potassium (I_A) conductance is modulated by MTII in RIPCre and POMC neurons

RIPCre (*B–E* and *G–J*) and POMC (*F*) neurons were voltage clamped and K^+ currents elicited following the pulse protocol shown in *A*. The 5 ms prepulse to −170 mV was used to deactivate any voltage-dependent potassium conductance. *B*, representative currents elicited by a −10 (upper traces; inset) and −15 mV (lower traces) voltage step in the absence (red) and presence of bath applied 4-AP (4 mM, blue). *C*, representative current families in the absence and presence of locally applied MTII (100 nM). *D* and *E*, MTII reversibly decreased the peak current, shown for expanded single test pulses to −20 mV (*D*) and with respect to time (*E*). Control currents are shown in blue, MTII in red, washout in black (*D*) and correspond to the time points displayed by these colours in *E*. *F*, representative currents elicited by a −20 mV voltage step in the absence (blue) and presence (red) of locally applied MTII (100 nM). *G*, control currents in the absence (left) and presence (right) of 100 nM r-heteropodatoxin-2 (HpTX). *H*, isolated I_A currents are shown in the absence (left) and presence of MTII (right), following subtraction of the I_K conductance isolated by HpTX (*G*, right). *I*, I_A currents evoked at −20 mV are shown following 5 s prepulses from −100 to −40 mV (10 mV increments). Note currents following the −40 mV prepulse were used to subtract the underlying I_K conductance. *J*, plots of voltage against the mean ratio of conductance (*G*) and maximum conductance (G_{max}) for each current in the absence (black symbols) and presence (red symbols) of MTII. Activation (squares) and steady-state inactivation (circles) curves shown were best fitted to the Boltzmann function and indicate the presence of a small window current that peaks at approximately −50 mV.

I_A peak amplitude, an action that is reversible and can be replicated by further application of MTII (Fig. 5*D* and *E*). Thus, at a test potential of −20 mV, MTII decreased I_A peak amplitude in RIPCre ($P < 0.05$, $n = 8$) neurons by 11 ± 5% ($n = 7$ out of 8) and in POMC ($P < 0.05$, $n = 8$) neurons by 10 ± 2% ($n = 5$ out of 8; Fig. 5*F*). These data indicate that MTII preferentially modulates the 4-AP-sensitive, voltage-dependent transient conductance I_A in both RIPCre and POMC neurons. To examine the mechanisms of action in more detail, we isolated I_K pharmacologically by removing I_A with a specific Kv4.2 toxin HpTX (100 nM, Tang *et al.* 2005; Fig. 5*G* and *H*, $n = 3$) or used a −40 mV prepulse to inactivate I_A (Fig. 5*I*, $n = 4$). Following the subtraction of I_K from the original current traces, the underlying I_A conductance was obtained (Fig. 5*H* and *I*). Although local application of MTII reduced the magnitude of I_A ($P = 0.05$, $n = 13$) by 23 ± 3% ($n = 7$ out 13), transient inactivation was not affected (at −20 mV, the inactivation time constants were 23 ± 6 ms in control *versus* 26 ± 7 ms in the presence of 100 nM MTII, $n = 7$). Modulation of the voltage-dependent activation and steady-state inactivation kinetics of I_A are possible mechanisms to explain the actions of MTII. Thus, voltage was plotted against the ratio of the I_A conductance (G) at each voltage and the maximum I_A conductance (G_{max}) and curves fitted to the Boltzmann function (Fig. 5*J*). However, the voltage-dependent activation and steady-state inactivation curves were not altered by MTII, in cells where I_A was reduced, with half-maximum activation ($V_{0.5}$) potentials of −31 ± 1 and −32 ± 1 mV ($n = 7$) for control and 100 nM MTII, respectively, and half-maximum inactivation ($V_{0.5}$) values of −65 ± 2 and −64 ± 2 mV ($n = 4$) for control and in the presence of 100 nM MTII, respectively. Note the presence of a small I_A window current, which peaks at approximately −50 mV (Fig. 5*J*) and encompasses the range of membrane potentials observed in this study. This is consistent with I_A participating in the control of the resting membrane potential.

In contrast with MTII, local application of 10 nM AgRP to voltage-clamped RIPCre neurons caused an increase in I_A amplitude ($P < 0.05$, $n = 9$) at all potentials where this current was visible (Fig. 6*A*). This action of AgRP was not immediately reversed on washout (Fig. 6*B* and *C*). For example, at a potential of −15 mV, AgRP increased peak amplitude by 19 ± 7% ($n = 7$ out of 9). Although on some occasions AgRP apparently increased the current through I_K (Fig. 6*A*), this was not a consistent finding and, on average, there was no significant effect on the steady-state outward current amplitude in the presence of either MTII or AgRP. As with MTII, the voltage-dependent activation curve of I_A was not affected by AgRP such that $V_{0.5}$ values were unaltered (control, −31 ± 1 mV; AgRP, −32 ± 1 mV, $n = 7$; Fig. 6*D*). These data suggest that MTII and AgRP modulate I_A independent of changes in voltage-dependent gating.

As previously described for POMC neurons (Roseberry *et al.* 2004), we found that the K_{IR} conductance in RIPCre arcuate neurons was extremely small (0.3 ± 0.1 nS, $n = 9$) under our recording conditions where the K_{ATP} channels were mostly closed. To increase the magnitude of the inward rectifier potassium conductance, the external potassium concentration was raised from 2.5 to 20 mM and RIPCre neurons were voltage clamped at −70 mV with 1 s voltage ramps from −170 to +30 mV used to assess the K_{IR} conductance. As a result of the relative linearization of the potassium gradient and the shift in the reversal potential (predictions from the Nernst equation are −106 and −51 mV for 2.5 and 20 mM $[K^+]_o$, respectively), the linear slope conductance (measured between −130 and

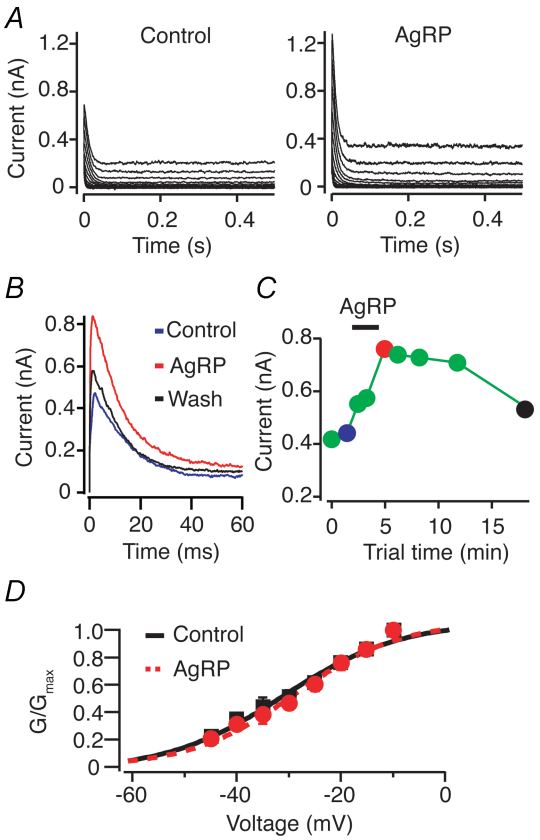

Figure 6. AgRP enhances the transient voltage-gated potassium conductance in RIPCre neurons
A, representative current families in the absence and presence of locally applied AgRP (10 nM). *B* and *C*, AgRP increased peak current amplitude, which was partially reversed on washout, shown for expanded single test pulses to −20 mV (*B*) and with respect to time (*C*). Control currents are shown in blue, AgRP in red, washout in black (*B*) and correspond to the time points displayed by these colours in *C*. *D*, plot of voltage against the mean ratio of conductance (G) and maximum conductance (G_{max}) for each current in the absence (black squares) and presence (red circles) of AgRP. Curves shown are the data best fitted to the Boltzmann function.

−50 mV) in 20 mM $[K^+]_o$ was 1.57 ± 0.23 nS ($n = 23$). A pronounced inward rectification close to the predicted reversal potentials was seen (Fig. 7*A*). In agreement with a previous study on arcuate neurons (Roseberry *et al.* 2004), this resting K_{IR} conductance was blocked by 100 μM external Ba^{2+}, which induced a 66 ± 10% ($P < 0.05$; $n = 5$ out of 5) reduction (Fig. 7*A* and *B*). In contrast, a much smaller proportion of K_{IR} was blocked by 200 μM tolbutamide, although this did not reach significance at the 95% level with a 26 ± 21% ($P = 0.09$, $n = 5$ out of 5) reduction in K_{IR} (Fig. 7*B*). It is surprising that application of the high affinity G-protein-coupled inward rectifier potassium (GIRK; Kir3 family) channel inhibitor (Kanjhan *et al.* 2005; Acuna-Goycolea & van den Pol, 2005) r-tertiapin-Q toxin (100 nM) had no significant effect (Fig. 7*C*) on the K_{IR} conductance (92 ± 6% of control, $P = 0.3$; $n = 5$) suggesting lack of resting GIRK channel activity under non-stimulatory conditions. Local application of 100 nM MTII had no effect on the linear slope conductance of K_{IR} ($P > 0.1$, $n = 26$), although in a minority population ($n = 10$ out of 26), a small (5.5 ± 2.0%) reversible decrease in current was observed (Fig. 7*D*). Likewise, K_{IR} slope conductance was not affected following the application of 10 nM AgRP (101 ± 4% of control, $P > 0.7$, $n = 13$, Fig. 7*E*).

We next assessed the actions of selective MC3 and MC4 receptor agonists on these potassium currents. We were concerned that the small changes we expected in I_A amplitude could be affected by errors that occur when trying to voltage clamp large amplitude currents. Therefore, to obviate this problem, we monitored both I_A and K_{IR} in the high (20 mM) $[K^+]_o$ solution, such that the shift in the predicted reversal potential increases inward (below −51 mV) and decreases outward (above −51 mV) potassium currents. Local application of the MC3R selective agonist 10 nM D-Trp^8-γ-MSH reduced the peak amplitudes of I_A ($P < 0.05$, $n = 12$, Fig. 7*F*), as did the MC4R selective agonist, 10 nM (cyclo(β-Ala-His-D-Phe-Arg-Trp-Glu)-NH_2) ($P < 0.05$, $n = 14$, Fig. 7*I*). Thus, at a test voltage of −15 mV, I_A peak amplitude was decreased by 8 ± 3% ($n = 8$ out of 12) and 12 ± 3% ($n = 7$ out of 14) in the presence of the MC3 (Fig. 7*G*) and MC4 (Fig. 7*J*) receptor agonists, respectively. Furthermore, the selective MC3R ($P < 0.05$, $n = 12$) and MC4R ($P = 0.07$, $n = 14$) agonists decreased K_{IR} currents (Fig. 7*F* and *I*), although the latter response was not significant at the 95% level of confidence. For RIPCre neurons that produced a response to these agonists, the steady-state slope conductance (measured at the end of each voltage step between −90 and −50 mV) was decreased by 18 ± 5% ($n = 8$ out 12) and 28 ± 8% ($n = 7$ out of 14) by application of the MC3 (Fig. 7*H*) and MC4 (Fig. 7*K*) receptor agonists, respectively. These data indicate that both melanocortin receptor subtypes contribute to melanocortin agonist modulation of I_A and perhaps K_{IR} conductances in ARC neurons.

Discussion

Melanocortin-driven excitation and inhibition of identified arcuate neurons

Previous studies demonstrate a wide CNS distribution of MC3R and MC4R, with moderate MC3R and low MC4R density in the arcuate (Mountjoy *et al.* 1994; Harrold *et al.* 1999; Liu *et al.* 2003). The PVN and dorsomedial nucleus (DMH) express much higher levels of MC4R (Liu *et al.* 2003) and are the hypothalamic areas with the greatest sensitivity to melanocortin agonists and AgRP (Kim *et al.* 2000). The location and effectiveness of MC4R modulation in hypothalamic circuits is particularly important given that MC4R knockout mice display a more severe obese phenotype (Huszar *et al.* 1997) than MC3R knockout mice (Butler *et al.* 2000). Moreover, AgRP and MTII do not significantly affect food intake or body weight in MC4R knockout mice (Fekete *et al.* 2004). It is interesting that using a Cre-mediated reactivation approach, Balthasar *et al.* 2005) showed that MC4R outside the PVN and amygdala is required to replicate the phenotype of the MC4R global null mouse. Clearly, MC4R is crucial for energy homeostasis, but questions remain as to the cellular mechanisms by which melanocortin agonists and AgRP modulate hypothalamic neuron excitability and the role of these receptors in the ARC.

We have demonstrated that two distinct arcuate neuron populations, POMC and RIPCre, display sensitivity to MC3R and MC4R selective agonists and to the inverse agonist, AgRP. A previous study on POMC neurons reported that the selective MC3R agonist D-Trp^8-γ-MSH hyperpolarized the majority of POMC neurons, although it was unclear whether this was due to indirect (MC3R autoreceptor) or direct action (Cowley *et al.* 2001). As we had previously reported that the mixed MC3R/MC4R agonist MTII depolarized RIPCre neurons (Choudhury *et al.* 2005), we expected the MC4R agonist to depolarize these arcuate neurons. However, MC3R and MC4R agonists depolarize both POMC and RIPCre neurons, and MTII induces depolarization in the presence of TTX. Furthermore, we found no evidence of altered synaptic drive (inhibitory or excitatory), causing a change of membrane potential, or of direct hyperpolarization of POMC neurons. These results are consistent with a recent report that MTII depolarizes MC4R-positive neurons in the DMH/PVN (Liu *et al.* 2003). Nevertheless, we observed that MTII drives a small increase in mIPSC amplitude in POMC neurons, indicating that under specific ionic conditions, MTII could hyperpolarize POMC neurons via an indirect, presynaptic mechanism. However, MTII failed to hyperpolarize POMC or RIPCre neurons under

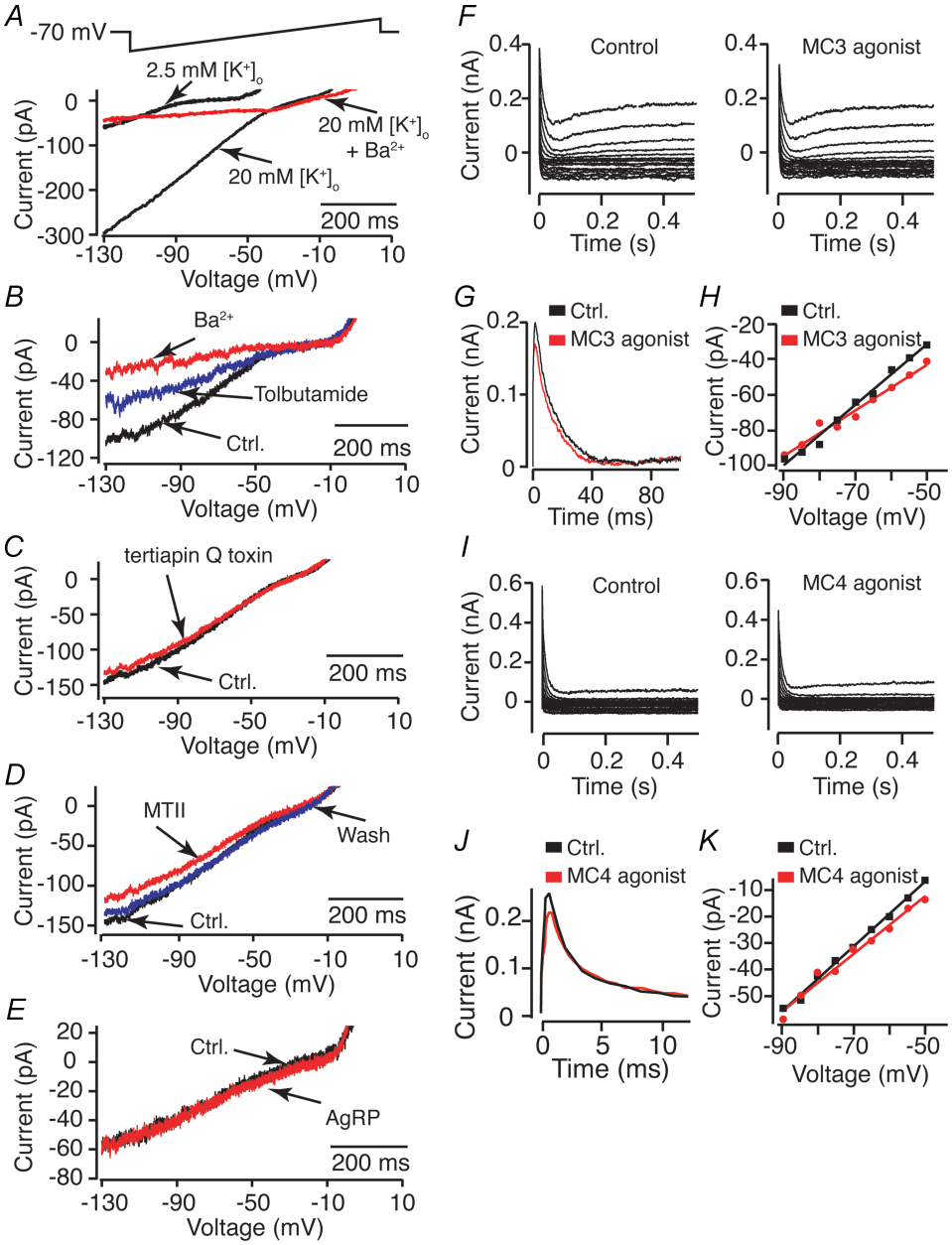

Figure 7. Melanocortin agonists modulate both K_{IR} and I_A
A, inward rectifying potassium conductance was monitored in voltage clamped RIPCre neurons by application of a 1 s voltage ramp (as shown). Increasing the potassium concentration from 2.5 to 20 mM increases the linear slope conductance and shifts the reversal potential to positive potentials. Note the pronounced inward rectification at the predicted Nernst potentials (2.5 mM $[K^+]_o$, −106 mV; 20 mM $[K^+]_o$, −51 mV). *B* and *C*, this inwardly rectifying potassium conductance was blocked by 100 μM Ba^{2+} (red traces in *A* and *B*), partly blocked by 200 μM tolbutamide (*B*, blue trace) but not by 100 nM r-tertiapin-Q toxin (*C*, red trace). *D* and *E*, local application of 100 nM MTII (*D*, red trace) reversibly (*D*, blue trace) decreased this current, although 10 nM AgRP had no affect (*E*, red trace). *F*, representative current families in the absence and presence of 10 nM MC3R agonist. *G*, the MC3 agonist decreased the peak I_A current, shown for expanded single test pulses to −15 mV. *H*, current–voltage relationships for steady-state current (measured at the end of the trace in *F*) in the absence (black squares) and presence (red circles) of the MC3 agonist. *I*, representative current families in the absence and presence of 10 nM MC4R agonist. *J*, the MC4 agonist decreased the peak I_A current, shown for expanded single test pulses to −10 mV. *K*, current–voltage relationships for steady-state current (measured at the end of the traces in *I*) in the absence (black squares) and presence (red circles) of the MC4 agonist.

control conditions or when the MC receptor signalling system in the postsynaptic neuron was blocked with Rp-cAMP. Following dialysis of the neuron with our internal recording solution (chloride reversal potential is −53 mV), an increase in $GABA_A$ activity is unlikely to have much influence on membrane potential (V_m, −50 mV). Using the perforated-patch technique, which does not disrupt the intracellular environment, we observed similar MTII-induced depolarizations. Increasing mIPSC amplitude could reduce input resistance and shunt the resting potassium conductance, which would result in depolarization. However, no significant change in input resistance was observed in this study, perhaps due to the combination of opening $GABA_A$ channels, inhibition of resting potassium conductances, and opening of voltage-gated conductances that accompany neuronal depolarization.

Does MC4R constitutive activity contribute to neuron excitability?

The MC4R displays constitutive activity in the absence of ligand, which is inhibited by AgRP binding (Nijenhuis *et al.* 2001). The long-term increase in food intake induced by AgRP administration may be a result of its inverse agonist properties because JKC363 (a selective MC4R antagonist) does not replicate this action (Kim *et al.* 2002). POMC and RIPCre neuronal hyperpolarization by AgRP in the absence of exogenously applied melanocortin agonist is consistent with inverse agonism, whereby the intrinsic activity of the receptor contributes a tonic depolarizing influence. Alternative explanations for the hyperpolarization are that AgRP acts on a separate (non-melanocortin) receptor (Hagan *et al.* 2000; Kim *et al.* 2002) or behaves as a competitive antagonist at MC3R and MC4R (Yang *et al.* 1999) to block the actions of endogenously released α-MSH. The latter possibility, although supported by the observation that SHU9119 causes RIPCre neuron hyperpolarization, is not substantiated by the lack of effect of JKC363, and the finding that AgRP induces hyperpolarization in the presence of TTX.

Mechanisms of melanocortin and AgRP actions on POMC and RIPCre neurons

The K^+ channel blocker data indicate that reduced postsynaptic potassium conductance underlies the depolarization elicited by melanocortin agonists. Voltage-clamp recordings from arcuate neurons demonstrate that melanocortin agonists reduced I_A and, to a lesser extent, K_{IR} conductances. Indeed, to completely inhibit the depolarizing/excitatory influence of MTII on RIPCre and POMC neurons required the simultaneous presence of inhibitors of these conductances, 4-AP (I_A) and Ba^{2+} (K_{IR}). This supports the notion that multiple K^+ conductances control the excitability of arcuate neurons. Previous studies have suggested that GIRK channels underlie the resting potassium conductance in POMC neurons (Cowley *et al.* 2001; Ibrahim *et al.* 2003; Roseberry *et al.* 2004). However, the concentrations ($> 100\ \mu$M) of barium used to substantiate this claim block most of the K_{IR} family. Indeed, the GIRK channel inhibitor r-tertiapin-Q toxin did not block the resting inward rectifier conductance in this, and a recent (Acuna-Goycolea & van den Pol, 2005), study indicating that another strong inward rectifier (e.g. KIR2 family) may underlie this conductance. The finding that melanocortin agonists, and AgRP, alter I_A in POMC and RIPCre neurons indicates that this conductance is a common target for transmitter receptors in hypothalamic neurons (Burdakov & Ashcroft 2002; Tang *et al.* 2005). The mechanism by which melanocortin receptors alter I_A is unclear. We have no evidence for modulation of voltage-dependent gating to explain the modification of I_A and suggest that a change in channel open state probability or availability may be responsible.

Arcuate neurons have high input resistances (1–2 GΩ) as a result of a very low resting conductance, thus a change of a few picoamps in resting K_{IR} and/or I_A window current is more than sufficient to produce millivolt changes in V_m. Additionally, because these neurons have a membrane potential that straddles the threshold for action potential firing, such modest changes in conductance and membrane potential can have a significant effect on spike frequency. A recent report shows that although NPY and peptide YY ($PYY_{3\text{-}36}$) inhibited resting calcium conductances in POMC and NPY neurons, this did not affect membrane potential (Acuna-Goycolea & van den Pol, 2005). However, NPY, $PYY_{3\text{-}36}$ and μ-opioid receptor stimulation activate a GIRK, r-tertiapin-Q toxin-sensitive (Acuna-Goycolea & van den Pol, 2005) conductance in identified arcuate neurons (Cowley *et al.* 2001; Ibrahim *et al.* 2003; Roseberry *et al.* 2004). This causes significant hyperpolarization with a large increase in resting potassium conductance. Consequently, to repolarize arcuate neurons when GIRK channels are activated, significant neuronal excitation or the closure of GIRK channels is required. Such responses are quite distinct from melanocortin receptor agonist actions described here, which use alternative conductances (I_A and K_{IR}) to produce modest changes in membrane potential (∼5 mV) and resting conductance (∼20% of control), and perhaps are best described as neuromodulatory rather than having the ability to turn neurons 'on' or 'off'.

Implications for the local arcuate circuit model

The presence of functional MC4R and MC3R on POMC neurons suggests that both could amplify melanocortin

peptide release, in a local arcuate positive feedback circuit. In contrast, AgRP acting on POMC neurons would inhibit this positive feedback loop, by antagonism of MC3R and through inverse agonism at MC4R, and provide local inhibition of the melanocortin network even in the absence of significant α-MSH release. This would reinforce orexigenic outputs and limit satiety signals at the level of the arcuate circuitry in addition to AgRP limiting melanocortin signals at second-order neurons in the PVN and LHA. The functional activation of melanocortin receptors on RIPCre neurons suggest that this neuronal type may also integrate the gene products locally released from both POMC- and AgRP-expressing neurons. Therefore, we suggest that the two-neuron model of ARC circuitry involved in control of energy homeostasis (Cowley *et al.* 2001; Cowley, 2003; Cone, 2005) may need to be extended in order to encompass additional neuronal types such as RIPCre.

References

Acuna-Goycolea C & van den Pol AN (2005). Peptide YY3-36 inhibits both anorexiogenic proopiomelanocortin and orexigenic neuropeptide Y neurons: implications for hypothalamic regulation of energy homeostasis. *J Neurosci* **25**, 10510–10519.

Balthasar N, Dalgaard LT, Lee CE, Yu J, Funahashi H, Williams T *et al.* (2005). Divergence of melanocortin pathways in the control of food intake and energy expenditure. *Cell* **123**, 493–505.

Bays HE (2004). Current and investigational anti-obesity agents and obesity therapeutic treatment targets. *Obes Res* **12**, 1197–1211.

Bednarek MA, MacNeil T, Tang R, Kalyani RN, van der Ploeg LH & Weinberg DH (2001). Potent and selective peptide agonists of α-melanotropin action at human melanocortin receptor 4: their synthesis and biological evaluation *in vitro*. *Biochem Biophys Res Commun* **286**, 641–645.

Bonilla C, Panguluri RK, Taliaferro-Smith L, Argyropoulos G, Chen G, Adeyemo AA *et al.* (2006). Agouti-related protein promoter variant associated with leanness and decreased risk for diabetes in West Africans. *Int J Obes* **30**, 715–721.

Burdakov D & Ashcroft FM (2002). Cholecystokinin tunes firing of an electrically distinct subset of arcuate nucleus neurons by activating A-type potassium channels. *J Neurosci* **22**, 6380–6387.

Butler AA, Kesterson RA, Khong K, Cullen MJ, Pelleymounter MA, Dekoning J, Baetscher M & Cone RD (2000). A unique metabolic syndrome causes obesity in the melanocortin-3 receptor-deficient mouse. *Endocrinology* **141**, 3518–3521.

Choudhury AI, Heffron H, Smith MA, Al-Qassab H, Xu AW, Selman C *et al.* (2005). The role of insulin receptor substrate 2 in hypothalamic and β cell function. *J Clin Invest* **115**, 940–950.

Cone RD (2005). Anatomy and regulation of the central melanocortin system. *Nat Neurosci* **8**, 571–578.

Cowley MA (2003). Hypothalamic melanocortin neurons integrate signals of energy state. *Eur J Pharmacol* **480**, 3–11.

Cowley MA, Smart JL, Rubinstein M, Cerdán MG, Diano S, Horvath TL, Cone RD & Low MJ (2001). Leptin activates anorexigenic POMC neurons through a neural network in the arcuate nucleus. *Nature* **411**, 480–484.

Dhillon H, Zigman JM, Ye C, Lee CE, McGovern RA, Tang V *et al.* (2006). Leptin directly activates SF1 neurons in the VMH, and this action by leptin is required for normal body-weight homeostasis. *Neuron* **49**, 191–203.

Erickson JC, Clegg KE & Palmiter RD (1996). Sensitivity to leptin and susceptibility to seizures of mice lacking neuropeptide Y. *Nature* **381**, 415–418.

Fan W, Boston BA, Kesterson RA, Hruby VJ & Cone RD (1997). Role of melanocortinergic neurons in feeding and the agouti obesity syndrome. *Nature* **385**, 165–168.

Farooqi IS, Yeo GS, Keogh JM, Aminian S, Jebb SA, Butler G, Cheetham T & O'Rahilly S (2000). Dominant and recessive inheritance of morbid obesity associated with melanocortin 4 receptor deficiency. *J Clin Invest* **106**, 271–279.

Fekete C, Marks DL, Sarkar S, Emerson CH, Rand WM, Cone RD & Lechan RM (2004). Effect of agouti-related protein in regulation of the hypothalamic-pituitary-thyroid axis in the melanocortin 4 receptor knockout mouse. *Endocrinology* **145**, 4816–4821.

Graham M, Shutter JR, Sarmiento U, Sarosi I & Stark KL (1997). Over-expression of Agrt leads to obesity in transgenic mice. *Nat Genet* **17**, 273–274.

Gropp E, Shanabrough M, Borok E, Xu AW, Janoschek R, Buch T *et al.* (2005). Agouti-related peptide-expressing neurons are mandatory for feeding. *Nat Neurosci* **8**, 1289–1291.

Hagan MM, Rushing PA, Pritchard LM, Schwartz MW, Strack AM, Van der Ploeg LH, Woods SC & Seeley RJ (2000). Long-term orexigenic effects of AgRP-(83–132) involve mechanisms other than melanocortin blockade. *Am J Physiol Regul Integr Comp Physiol* **279**, R47–R52.

Harrold JA, Widdowson PS & Williams G (1999). Altered energy balance causes selective changes in melanocortin-4 (MC4-R), but not melanocortin-3 (MC3-R), receptors in specific hypothalamic regions: further evidence that activation of MC4-R is a physiological inhibitor of feeding. *Diabetes* **48**, 267–271.

Haskell-Luevano C & Monck EK (2001). Agouti-related protein functions as an inverse agonist at a constitutively active brain melanocortin-4 receptor. *Regul Pept* **99**, 1–7.

Hille B (2001). *Ion Channels of Excitable Membrane*, 3rd edn. Sinauer Associates Inc., Massachusetts, USA.

Huszar D, Lynch C, Rair-Huntress V, Dunmore JH, Fang Q, Berkemeier LR *et al.* (1997). Targeted disruption of the melanocortin-4 receptor results in obesity in mice. *Cell* **88**, 131–141.

Ibrahim N, Bosch MA, Smart JL, Qiu J, Rubinstein M, Rønnekleiv OK, Low MJ & Kelly MJ (2003). Hypothalamic proopiomelanocortin neurons are glucose responsive and express K_{ATP} channels. *Endocrinology* **144**, 1331–1340.

Kanjhan R, Coulson EJ, Adams DJ & Bellingham MC (2005). Tertiapin-q blocks recombinant and native large conductance K^+ channels in a use-dependent manner. *J Pharmacol Exp Ther* **314**, 1353–1361.

Kas MJ, van Dijk G, Scheurink AJ & Adan RA (2003). Agouti-related protein prevents self-starvation. *Mol Psychiatry* **8**, 235–240.

Kim MS, Rossi M, Abbott CRAI, Ahmed SH, Smith DM & Bloom SR (2002). Sustained orexigenic effect of Agouti related protein may not be mediated by the melanocortin receptor. *Peptides* **23**, 1069–1076.

Kim MS, Rossi M, Abusnana S, Sunter D, Morgan DG, Small CJ *et al.* (2000). Hypothalamic localization of the feeding effect of agouti-related peptide and alpha-melanocyte-stimulating hormone. *Diabetes* **49**, 177–182.

Lechan RM & Tatro JB (2001). Hypothalamic melanocortin signaling in cachexia. *Endocrinology* **142**, 3288–3291.

Liu GX, Derst C, Schlichthörl G, Heinen S, Seebohm G, Brüggemann A, Kummer W, Veh RW, Daut J & Müller RP (2001). Comparison of cloned Kir2 channels with native inward rectifier K^+ channels from guinea-pig cardiomyocytes. *J Physiol* **532**, 115–126.

Liu H, Kishi T, Roseberry AG, Cai X, Lee CE, Montez JM, Friedman JM & Elmquist JK (2003). Transgenic mice expressing green fluorescent protein under the control of the melanocortin-4 receptor promoter. *J Neurosci* **23**, 7143–7154.

Mountjoy KG, Mortrud MT, Low MJ, Simerly RB & Cone RD (1994). Localization of the melanocortin-4 receptor (MC4-R) in neuroendocrine and autonomic control circuits in the brain. *Mol Endocrinol* **8**, 1298–1308.

Nijenhuis WA, Oosterom J & Adan RA (2001). AgRP (83-132) acts as an inverse agonist on the human melanocortin-4 receptor. *Mol Endocrinol* **15**, 164–171.

Plum L, Ma X, Hampel B, Balthasar N, Coppari R, Münzberg H *et al.* (2006). Enhanced PIP3 signaling in POMC neurons causes KATP channel activation and leads to diet-sensitive obesity. *J Clin Invest* **116**, 1886–1901.

Ramos EJ, Meguid MM, Campos AC & Coelho JC (2005). Neuropeptide Y, α-melanocyte-stimulating hormone, and monoamines in food intake regulation. *Nutrition* **21**, 269–279.

Roseberry AG, Liu H, Jackson AC, Cai X & Friedman JM (2004). Neuropeptide Y-mediated inhibition of proopiomelanocortin neurons in the arcuate nucleus shows enhanced desensitization in *ob/ob* mice. *Neuron* **41**, 711–722.

Srinivasan S, Lubrano-Berthelier C, Govaerts C, Picard F, Santiago P, Conklin BR & Vaisse C (2004). Constitutive activity of the melanocortin-4 receptor is maintained by its N-terminal domain and plays a role in energy homeostasis in humans. *J Clin Invest* **114**, 1158–1164.

Takano M & Ashcroft FM (1996). The Ba^{2+} block of the ATP-sensitive K^+ current of mouse pancreatic beta-cells. *Pflugers Arch* **431**, 625–631.

Tang SL, Tran V & Wagner EJ (2005). Sex differences in the cannabinoid modulation of an A-type K^+ current in neurons of the mammalian hypothalamus. *J Neurophysiol* **94**, 2983–2986.

Wang XY, McKenzie JS & Kemm RE (1996). Whole-cell K^+ currents in identified olfactory bulb output neurones of rats. *J Physiol* **490**, 63–77.

Wikberg JE (1999). Melanocortin receptors: perspectives for novel drugs. *Eur J Pharmacol* **375**, 295–310.

Yang YK, Thompson DA, Dickinson CJ, Wilken J, Barsh GS, Kent SB & Gantz I (1999). Characterization of agouti-related protein binding to melanocortin receptors. *Mol Endocrinol* **13**, 148–155.

Acknowledgements

We thank Dr G. Barsh for kindly providing the POMC mice and Dr V. J. Hruby for the gift of D-Trp^8-γ-MSH. Research support was provided by The Wellcome Trust (M.L.J.A. and D.J.W.), Medical Research Council (D.J.W.) and Biotechnology and Biological Sciences Research Council (D.J.W.).